

Up-Conversion of Phonons to Photons in a Mechanically Coupled Split-Post Resonator

Sonali Parashar, William M. Campbell, Jeremy Bourhill, Eugene Ivanov, Maxim Goryachev, and Michael E. Tobar

Abstract – We investigated a novel split-post re-entrant microwave cavity coupled to mechanical phonons in a bulk acoustic wave (BAW) resonator made of lithium niobate and a membrane resonator made of a single-crystal sapphire substrate. Unlike previous configurations, this setup employs a different coupling mechanism for the photonic element, thereby enhancing the spatial overlap between the microwave field and the acoustic mode—a critical factor for achieving stronger coupling. We present results of a lithium niobate BAW resonator placed inside a re-entrant cavity at approximately 4 K. The BAW and sapphire resonators were symmetrically located between the two posts of the split post resonator. In this configuration, BAW modes exhibited quality factors exceeding 10^6 . Various mode families were explored to characterize their respective coupling strengths. For the lithium niobate resonator, we measured an optomechanical coupling rate g_0 of 0.014 mHz for a longitudinal mode at 4.8 MHz. In comparison, a shear mode at 4.2 MHz exhibited a much lower coupling rate of 2.67×10^{-7} Hz, while the optimum coupling to the sapphire membrane is still under investigation. These results demonstrate the dependence of the coupling rate on the nature of the acoustic mode, with significantly stronger coupling observed for longitudinal modes. Moreover, this excitation mechanism achieves higher coupling rates compared to previously used techniques.

1. Introduction

Past studies exploring the fundamental interactions between photonic and phononic systems have advanced our understanding of quantum electrodynamics and its technological applications [1]. These systems enable the investigation of key quantum phenomena, such as parametric amplification [2], resolved sideband

Manuscript received 6 March 2025. This research was supported by the ARC Centre of Excellence for Engineered Quantum Systems (EQUS), CE170100009, and the Defence Science and Technology Group as part of the EQUS Quantum Clock Flagship program. Additional support was provided by the ARC Centre of Excellence for Dark Matter Particle Physics, CE200100008.

Sonali Parashar, William M. Campbell, Jeremy Bourhill, Eugene Ivanov, Maxim Goryachev, and Michael E. Tobar are with the Quantum Technologies and Dark Matter Labs. Department of Physics, University of Western Australia, 35 Stirling Highway, Crawley, WA 6009, Australia; email: sonali.parashar@research.uwa.edu.au, william.campbell@research.uwa.edu.au, jeremy.bourhill@uwa.edu.au, eugene.ivanov@uwa.edu.au, maxim.goryachev@uwa.edu.au, michael.tobar@uwa.edu.au.

cooling, and optomechanically induced transparency and absorption [3, 4]. Such effects are critical for probing fundamental quantum limits [5, 6] and have practical implications in gravitational wave detection [7, 8], dark matter searches [9], quantum communication, precision metrology, and quantum information processing and storage [10, 11].

Highly coherent optomechanical systems also support detection with parametric transducers, and the development of strongly coupled quantum readout technologies is essential for reducing noise floors and enabling coherent transduction [12]. These capabilities are particularly relevant for tests of quantum gravity, including proposals to detect individual gravitons [13]. Macroscopic mechanical resonators, especially in the milligram mass range, provide an excellent platform for exploring the quantum-to-classical transition in systems such as bulk acoustic wave (BAW) resonators and membranes.

2. Theory

The theory for the calculation of coupling rate is given by the interaction between a phonon and a photon mode, and the governing interaction Hamiltonian is given by (1) below,

$$H = \omega_c a^\dagger a + \omega_m b^\dagger b + g_0 (a^\dagger a) (b^\dagger + b) \quad (1)$$

Here a^\dagger is the creation operator, and a is the annihilation operator for photonic modes, with b^\dagger and b being the creation and annihilation operators for phonon modes. Where ω_c is the microwave cavity [MW] operating resonant frequency, and ω_m is the resonance frequency of the mechanical resonator.

Parametric detection is achieved by detecting the change in the microwave frequency caused by a coupled mechanical resonator. Here, the displacement “ x ” of the mechanical resonator upconverts the phonon transition in megahertz to a shift in microwave frequency at the gigahertz frequency range. This is presented in [1 eq. (2)]. The pull factor calculated from the experiments is given in (3) and is used to measure the coupling rate of an opto-mechanically coupled system g_0 , given in (4). However, (5) shows that for a linearly coupled system, the basic relationship between displacement and charge on the surface of BAW is used to experimentally evaluate the pull factor.

$$\omega_c(x) \approx \omega_c + x \frac{\delta\omega_c}{\delta x} + \dots \quad (2)$$

$$G = - \frac{\delta\omega_c}{\delta x} \quad (3)$$

$$g_0 = Gx_{zpf} \quad (4)$$

$$q = k_m^2 x \quad (5)$$

Here $x_{zpf} = \sqrt{2/(\omega_m M_{\text{eff},m})}$ is the zero-point fluctuation of the mechanical resonance, $M_{\text{eff},m}$ is the effective mode mass of the mechanical mode and is evaluated using COMSOL multi-physics Finite Element Method tool, and $k_m^2 = \frac{\omega_m M_{\text{eff},m}}{Q_m R_m}$ is a parameter given by the BAW mechanical element, where ω_m is the frequency of a given BAW mode, Q_m is the quality factor of the mechanical mode, and R_m is the effective resistance of the BAW mode on resonance [14].

To elaborate further, a BAW resonator may be modeled as a lumped LCR resonant circuit and is explained by the Butter worth-Van Dyke model, which could be understood from the BAW-resonator lumped circuit theory where different modes are modeled as having an effective impedance (L), capacitance (C), and resistance (R) value and are viewed as a parallel branch in the resonant circuit. Similarly, the characterization of lithium niobate BAW was performed, which led to the identification of the following two types of modes in these BAW devices: A-type (longitudinal) and B-type (shear) modes because it is a uniaxial crystal. The reason for the popularity of lithium niobate over other materials is its high-quality factor and low-loss tangent. The detailed low-loss characterization can be cited from [15].

3. Experimental Realization

The lithium niobate BAW, whose diameter is $\phi = 29$ mm, is modelled using COMSOL, where it is been placed inside the microwave resonator symmetrically between the two posts. The gap between the microwave post and the body of the microwave resonator is less than 0.5 mm. The current experiments were performed using a BAW resonator for longitudinal mode at $A_{3,0,0}$ and shear modes at $B_{5,0,0}$ [15]. The distinctive shape of the BAW lends itself to a unique phonon and mechanical mode distribution that aligns along the center of the material [7]. This centralization enhances the material's responsiveness when placed within the electric field of the microwave resonator, creating a more pronounced interaction and sensitivity.

Furthermore, the re-entrant microwave cavity was optimized for the cavity dimensions to maximize the resonator's form factor and quality factor [16]. The cavity is comprised of high-purity, oxygen-free copper. The microwave mode was characterized at room temperature (RT) and 4 K. The loaded quality factor Q_L for

the microwave cavity has been improved from 330 at RT to 2500 at 4 K. The input port was driven with an incident power of 0.1 mW. Microwave cavity modes were characterized via S_{21} parameter measurements using a vector network analyzer. The symmetrical two-post structure of the cavity concentrates the electricity at the center. The sapphire membrane was measured using the same setup (replacing the BAW resonator), the field at the center coinciding with the region of maximum mechanical mode amplitude in the BAW resonator. This configuration enhances the field overlap and yields a higher form factor [14].

Additionally, direct voltage biasing of the posts enables piezoelectric modulation of the BAW resonator. A homodyne detection technique configured as a phase bridge or frequency discriminator was employed to perform the measurements. The frequency discriminator was tuned to the fundamental mode of the microwave resonator, resonating at 6.02 GHz. Frequency shifts in the cavity, induced by coupling to mechanical modes, were detected by maintaining a quadrature condition between the local oscillator and radio frequency (RF) signals. This configuration ensures the system remains insensitive to amplitude noise, isolating frequency-dependent phase fluctuations. A microwave signal was injected using a frequency synthesizer, and the intermediate frequency (IF) output from the mixer containing the upconverted signal was monitored using a fast Fourier transform spectrum analyzer. Figure 1 provides a schematic of the experimental setup.

4. Results and Discussion

The results presented here correspond to the output signal from the mixer acquired using the homodyne detection scheme illustrated in Figure 1. This output reflects the frequency modulation of the microwave cavity induced by its coupling to mechanical modes due to the BAW or sapphire resonator. The observed signals were analyzed using a fast Fourier transform spectrum analyzer to extract spectral features and coupling characteristics. Below, we summarize the key experimental observations and findings derived from these measurements.

4.1 Coupling Rate Calculations

The coupling rate was determined by measuring the displacement “ x ” of the mechanical element, which was inferred from the induced current through each BAW mode in response to an applied voltage. This approach yields the displacement as described in (5). The resulting displacement shifts the microwave resonance frequency, as described by (3) and (4), and is detected using a homodyne phase bridge. Experimental results for the longitudinal mode at 4.8 MHz and the shear mode at 4.2 MHz are presented in Figure 2, showing the mixer output voltage corresponding to each mode's displacement. The experimentally measured

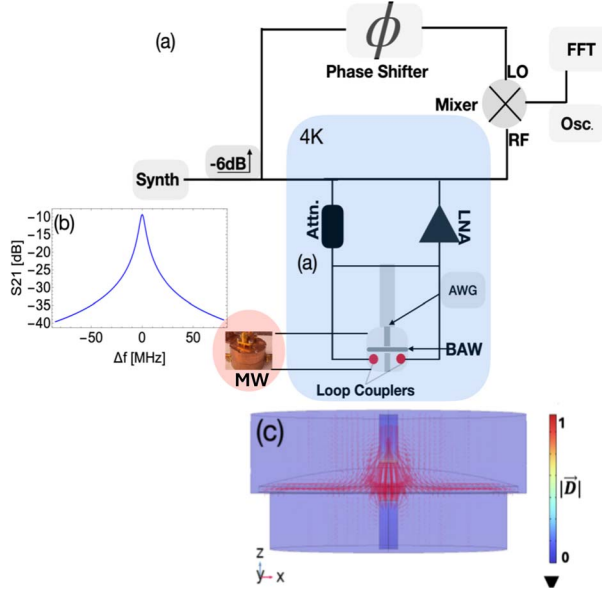


Figure 1. (a) The frequency discriminator setup used for the experiments at 4 K. The mixer output voltage was observed by the fast Fourier transform spectrum analyzer when a piezoelectric voltage was applied across BAW by using an arbitrary waveform generator (AWG). Where an attenuation (Attn.) of -30 dB is at the input line going to the cavity, and a low-noise amplifier (LNA) of 30 -dB gain at the output line of the cavity. (b) The measured S_{21} parameter for the fundamental microwave mode. (c) The magnitude of the \overline{D} -field inside the microwave cavity for the BAW readout. The sapphire membrane was measured using the same setup (replacing the BAW resonator).

coupling rates are 1.44×10^{-5} Hz for the longitudinal mode and 2.67×10^{-7} Hz for the shear mode. Detailed calculations can be found in [14].

In addition, we investigated the mechanical response of a 0.5 -mm thick sapphire membrane placed inside a split-post microwave resonator to probe its drum modes. The mixer output for a higher-order drum mode at 48.5 kHz is shown in Figure 3. In this setup, the sapphire membrane is driven by a piezo-actuator, and the signal is detected using a phase bridge readout. The purpose of this investigation is to show that the split-post resonator shows a quadratic nature of displacement when coupled with a drum mode, which is

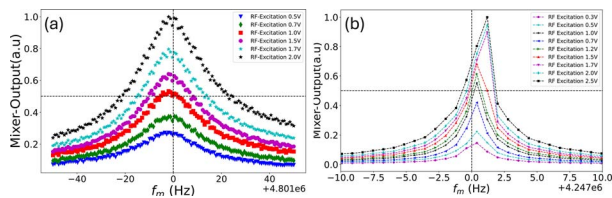


Figure 2. The normalized voltage output at the mixer IF port for different RF excitation voltages applied using an AWG was measured using a fast Fourier transform. (a) Mixer output voltages are shown for different RF excitation for a longitudinal mode of BAW at 4.8 MHz at 4 K. (b) Mixer output for different RF excitation of BAW for shear mode at 4.2 MHz at 4 K.

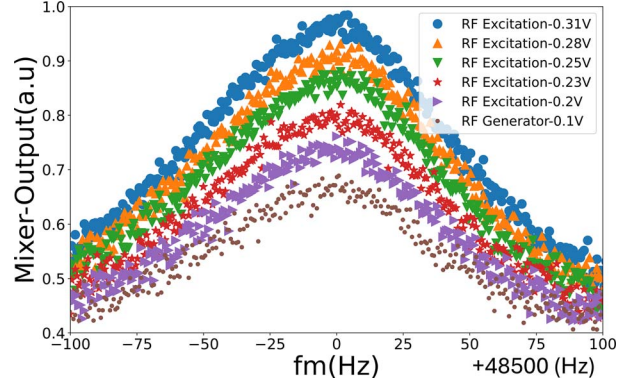


Figure 3. The normalized voltage output at the mixer IF port for different drive voltages (RF excitation) applied by the piezo actuator and the output from a split post is read using a homodyne detection technique by a fast Fourier transform for analyzing a sapphire drum mode at 48.5 kHz at RT.

due to the symmetric field profile inside a “split-post” resonator.

The coupling rates for the mechanical modes $A_{3,0,0}$ (4.8 MHz) and $B_{5,0,0}$ (4.2 MHz) in the BAW resonator are listed in Table 1. These results demonstrate promising coupling strengths for a resonator with mass in the milligram range, highlighting mode-dependent variations in coupling performance.

5. Conclusion

We investigated the coupling rates of various mechanical modes, both A type (longitudinal) and B type (shear), in a lithium niobate BAW resonator using a split-post microwave cavity. The analysis revealed distinct coupling behavior for A- and B-type modes. Of note, the coupling rate for the longitudinal $A_{3,0,0}$ mode was found to be approximately four times greater than previously reported values. This enhancement is largely attributed to the optimized geometry of the microwave resonator, which significantly improves the transduction efficiency. In addition to the BAW studies, we successfully implemented and read out the motion of a sapphire membrane resonator coupled to the same microwave structure. This work makes a significant contribution to the characterization of both BAW- and membrane-based mechanical resonators. It lays a strong foundation for future efforts aimed at developing highly coherent and sensitive readout architectures using microwave devices. Moreover, the results support further exploration into quadratic displacement sensitivity for membrane resonators,

Table 1. Coupling rates for frequencies, f_m for different mechanical mode frequencies in MHz for BAW mechanical resonator; here g_0 is the coupling rate in Hz and $u(g_0)$ is the uncertainty associated with these values in Hz

$X_{n,m,p}$	f_m (MHz)	g_0 (Hz)	$u(g_0)\%$
$A_{3,0,0}$	4.8	1.44×10^{-5}	0.8% (g_0)
$B_{5,0,0}$	4.2	2.67×10^{-7}	0.6% (g_0)

an important feature for probing a range of fundamental physical phenomena.

6. References

1. M. Aspelmeyer, T. J. Kippenberg, and F. Marquardt, "Cavity Optomechanics," *Reviews of Modern Physics*, **86**, 4, December 2014, pp. 1391–1452.
2. B. Cuthbertson, M. Tobar, E. Ivanov, and D. Blair, "Parametric Back-Action Effects in a High-Q Cryogenic Sapphire Transducer," *Review of Scientific Instruments*, **67**, July 1996, pp. 2435–2442.
3. J. Bourhill, E. Ivanov, and M. Tobar, "Precision Measurement of a Low-Loss Cylindrical Dumbbell-Shaped Sapphire Mechanical Oscillator Using Radiation Pressure," *Physical Review A*, **92**, August 2015, p. 023817.
4. J. Bourhill, N. d. C. Carvalho, M. Goryachev, S. Galliou, and M. E. Tobar, "Generation of Coherent Phonons via a Cavity Enhanced Photonic Lambda Scheme," *Applied Physics Letters*, **117**, October 2020, p. 164001.
5. M. Goryachev, Z. Kuang, E. N. Ivanov, P. Haslinger, H. Müller, et al., "Next Generation of Phonon Tests of Lorentz Invariance Using Quartz BAW Resonators," *IEEE Transactions on Ultrasonics, Ferroelectrics, and Frequency Control*, **65**, 6, June 2018, pp. 991–1000.
6. P. Bushev, J. Bourhill, M. Goryachev, N. Kukharchyk, E. Ivanov, et al., "Testing the Generalized Uncertainty Principle With Macroscopic Mechanical Oscillators and Pendulums," *Physical Review D*, **100**, September 2019, p. 066020.
7. M. Goryachev and M. E. Tobar, "Gravitational Wave Detection With High-Frequency Phonon Trapping Acoustic Cavities," *Physical Review D*, **90**, November 2014, p. 102005.
8. M. Goryachev, W. M. Campbell, I. S. Heng, S. Galliou, E. N. Ivanov, et al., "Rare Events Detected With a Bulk Acoustic Wave High Frequency Gravitational Wave Antenna," *Physical Review Letters*, **127**, 7, August 2021, p. 071102.
9. W. M. Campbell, B. T. McAllister, M. Goryachev, E. N. Ivanov, and M. E. Tobar, "Searching for Scalar Dark Matter via Coupling to Fundamental Constants With Photonic, Atomic, and Mechanical Oscillators," *Physical Review Letters*, **126**, February 2021, p. 071301.
10. A. Y. Cleland, E. A. Wollack, and A. H. Safavi-Naeini, "Studying Phonon Coherence With a Quantum Sensor," *Nature Communications*, **15**, June 2024, p. 4979.
11. P. Arrangoiz-Arriola, E. A. Wollack, M. Pechal, J. D. Witmer, J. T. Hill, et al., "Coupling a Superconducting Quantum Circuit to a Phononic Crystal Defect Cavity," *Physical Review X*, **8**, 3, July, 2018, p. 031007.
12. C. Locke, M. Tobar, E. Ivanov, and D. Blair, "Parametric Interaction of the Electric and Acoustic Fields in a Sapphire Monocrystal Transducer With a Microwave Readout," *Journal of Applied Physics*, **84**, December 1998, pp. 6523–6527.
13. G. Tobar, S. K. Manikandan, T. Beitel, and I. Pikovski, "Detecting Single Gravitons With Quantum Sensing," *Nature Communications*, **15**, August 2024, p. 7229.
14. S. Parashar, W. M. Campbell, J. Bourhill, E. N. Ivanov, M. Goryachev, et al., "Upconversion of Phonon Modes Into Microwave Photons in a Lithium Niobate Bulk Acoustic Wave Resonator Coupled to a Microwave Cavity," *APL Photonics*, **9**, 11, November 2024, p. 111304.
15. W. M. Campbell, S. Parashar, M. E. Tobar, and M. Goryachev, "Low Temperature Properties of Low-Loss Macroscopic Lithium Niobate Bulk Acoustic Wave Resonators," preprint arXiv:2407.17693, July 2024.
16. J.-M. Le Floch, Y. Fan, M. Aubourg, D. Cros, N. C. Carvalho, et al., "Rigorous Analysis of Highly Tunable Cylindrical Transverse Magnetic Mode Re-Entrant Cavities," *The Review of Scientific Instruments*, **84**, 12, December 2013, p. 125114.